



Effects and Mechanism of Two Nanoparticles (Titanium Dioxide and Silver) to *Moina mongolica* Daday (Crustacea, Cladocera)

Jianrong Huang, Shaojing Li and Yuanshao Lin*

College of Ocean and Earth Sciences, Xiamen University, Xiamen, China

OPEN ACCESS

Edited by:

Jian Zhao,
Ocean University of
China, China

Reviewed by:

Fei Li,
Chinese Academy of
Sciences (CAS), China
Chuanxin Ma,
Guangdong University
of Technology, China

*Correspondence:

Yuanshao Lin
yslin@xmu.edu.cn

Specialty section:

This article was submitted to
Marine Pollution,
a section of the journal
Frontiers in Marine Science

Received: 02 April 2022

Accepted: 17 June 2022

Published: 27 July 2022

Citation:

Huang J, Li S and Lin Y (2022)
Effects and Mechanism of Two
Nanoparticles (Titanium Dioxide and
Silver) to *Moina mongolica* Daday
(Crustacea, Cladocera).
Front. Mar. Sci. 9:909701.
doi: 10.3389/fmars.2022.909701

The nearshore and estuary are the main gathering areas of nanoparticles (NPs), and salinity change is a crucial characteristic in these marine areas. *Moina mongolica* Daday is an important open-ended bait in the nearshore aquaculture environment. Investigating the toxicity mechanism of NPs to *M. mongolica* under different salinity conditions is crucial to exploring the biological impact of NPs in the nearshore environment. Two typical metal oxide and metal NPs of TiO₂ and Ag were used in this study to test the acute, chronic, and reproductive toxicities of *M. mongolica* (Cladocera) in marine environments of different salinity gradients. The toxic effects and mechanisms of the two NPs on *M. mongolica* were discussed by ecotoxicology and transcriptional analysis, respectively. A total of 27,274 genes were assembled, and 11,056 genes were successfully compared. Results suggested that TiO₂ and Ag NPs showed particle toxicity with oxidation generation and immune emergencies on *M. mongolica*. Compared with TiO₂, Ag NPs showed strong toxicity with reproductive toxicity due to the release of Ag⁺, resulting in a reduction in reproduction, which is a decrease in the number of offspring and the *rm*. Critical DEGs involved in carapace showed carapace damage of *M. mongolica*, due to adhesion and accumulation (approximately 40%–60% of all accumulation) on carapace, which was one of the toxic mechanisms of the two NPs. The salinity factor caused the aggregation of both NPs, and Ag⁺ release of Ag NPs. The toxicity of TiO₂ NPs to *M. mongolica* increases with salinity, but that of Ag NPs decreases.

Keywords: nanoparticles, titanium dioxide nanoparticles, silver nanoparticles, nanotoxicity, *Moina mongolica* Daday, transcriptional analysis

1 INTRODUCTION

Titanium dioxide nanoparticles (TiO₂ NPs) and silver nanoparticles (Ag NPs) are the two most widely used NPs due to the development of nanotechnology and the special physical and chemical properties in recent decades (Volker et al., 2013; Minetto et al., 2014; Khosravi-Katuli et al., 2017). TiO₂ NPs are increasingly used in cosmetics and antifouling coatings (Minetto et al., 2014), and Ag NPs are utilized in various antifungal materials (Griffitt et al., 2013). These NPs will eventually enter the marine environment through different compartments [air, soil, and water (Corsi et al., 2014)], which will likely result in lethal or adverse effects on environmental organisms and marine aquatic products (Griffitt et al., 2013; Kang et al., 2016; Magesky et al., 2016; Davarazar et al., 2021). Therefore,

studying the influence of the two NPs on marine organisms in the estuary and nearshore is necessary (Fajardo et al., 2022). Salinity is the most important and changing environmental factor in the estuary and nearshore, and salinity changes could affect the aggregation, size, and ion release of metal and metal oxide NPs in seawater (Rotini et al., 2017; Yung et al., 2017). Therefore, salinity change is a crucial factor affecting the toxicity of NPs in seawater (Yung et al., 2015; Rotini et al., 2017).

The class of cladocerans are good model organisms available for NP ecotoxicity tests because they are filter-feeding zooplankton crustaceans (Griffitt et al., 2008; Matranga and Corsi, 2012). Moreover, their participation in energy transfer and nutrient regeneration as key herbivores in the food web is a crucial biogeochemical role in ecosystems (Spicer, 2013). The current study selected the cladoceran *M. mongolica*, an indigenous and ecologically important halophilic species in the southeastern part of China, which is widely used as a nutritious live food source for the fish and developing larvae of a variety of marine economic farming species (He et al., 2001). *M. mongolica* with characteristics, such as an approximate size (1.0–1.4 mm long and 0.8 mm wide), was easy to culture under laboratory conditions. The short but predictable life cycle and high fecundity of *M. mongolica* make it a good and cost-effective indicator for studying the biological effects of NPs (Wang et al., 2016). This species can also be investigated for acute and reproduction toxicity tests considering the relative species *Daphnia* based on the guidelines of OECD 202 (OECD, 2004) and OECD 211 (OECD, 2012).

Recent studies have shown that metals and metal oxide NPs have adverse influence on aquatic animals, which may lead to toxicity including death, intestinal blockage, oxidative stress, and DNA damage (Paterson et al., 2011; Griffitt et al., 2013; Ivask et al., 2014; Adam et al., 2015; Gong et al., 2016; Pan et al., 2018; Du et al., 2021). Current evidence suggests that the toxicity of metal and metal oxide NP factors include material, size, surface area, agglomeration, and dissolved release or vectorization effect reactivity (Asharani et al., 2008; Gagné et al., 2012; Volker et al., 2013; Châtel and Mouneyrac, 2017; Orbea et al., 2017). Compared with freshwater, the complexity of the seawater environment, such as the ionic strength (IS) of salinity seawater, would cause the agglomeration and precipitation of NPs. Such complexity decreases the concentration of NPs in suspension and reduces the potential contact frequency of NPs (Zhu et al., 2011); it may also influence the generation of ions of metal-based NPs (Quik et al., 2011; Brunelli et al., 2013). NP aggregates, such as TiO₂ NPs, were filled inside the digestive tracts of *Artemia salina*, leading to oxidative stress due to impaired food uptake (Ates et al., 2013). The aggregate and size of TiO₂ NPs were also inversely proportional to the toxicity effects toward marine rotifers (Auffan et al., 2009; Clément et al., 2013). Metal and metal oxide NP release ions, such as ionic silver (Ag⁺) release, were typically identified to be at least partly responsible for the toxicity of Ag NPs (Scanlan et al., 2013); NP aggregates adhered to the carapace of marine organisms (Yung et al., 2015; Corsi et al., 2020). Nevertheless, it remains unclear how salinity factors affect damage of carapace adhesion and the toxicity (particle and ionic toxicity) of NPs on marine organisms.

The carapace mainly consists of cuticle protein and chitin in cladocerans, which play an important role in external environmental defense, reproduction, growth, etc. (Repka et al., 1995; Liu et al., 2014). However, little is known about the effect and mechanism of NP aggregates adhering to the carapace, as well as the effect of salinity. This study investigates the effects of acute and chronic exposure by comparing the survival, reproduction, and other parameters and examining the response transcriptomics level. The current study also reveals the effect and mechanism of salinity change on the toxicity of two NPs in saltwater organisms. Thus, this study could be applied in the early detection of ecologic risks mediated by other organisms and assessment of the safety of metal-based NPs for use in seawater.

2 MATERIALS AND METHODS

2.1 Chemicals

The uncoated TiO₂ NP powder (≥99.5% trace metal basis, cat. #13463-67-7-5G) and Ag NPs (≥99% trace metal basis, cat. #484059-5G) were purchased from Sigma-Aldrich Sigma-Aldrich, USA. Ultrapure water (18.2M Ω cm, Spring-R10i) was provided by a Millipore Advantage System (Merck Millipore, Darmstadt, Germany). Oshima's artificial seawater (Oshima's ASW, salinity 30‰) was prepared by dissolving NaCl (28 g), KCl (0.8 g), MgCl₂·6H₂O (5 g), and CaCl₂·H₂O (1.2 g) in 1 l ultrapure water and subsequently adjusting the pH to 8.0 ± 0.1 with 0.5 M NaOH. A 0.22- μ m microporous membrane (Merck Millipore Ltd., Burlington, MA, USA) was used for filtration after stirring and fully aerating for 24 h (dissolved oxygen >8.6 mg/l), and deionized water was then utilized to facilitate dilution to the required salinity (5‰, 15‰, 25‰, and 35‰).

The nanoparticle suspension stock dispersion of TiO₂ NPs (500 mg/l) and Ag NPs (100 mg/l) was prepared, and ultrasonic vibration was used for 40 min (100 kHz, KQ-250DE). These NPs were then transferred to a brown bottle for use (protect from light). The nanoparticle suspension stocks of TiO₂ NPs (500 mg/l) and Ag NPs (100 mg/l) were used to realize dilution to the required concentration. The nanoparticle suspension stock was then ultrasonically shaken for 30 min before dilution. The solution used for dilution was prepared in advance and fully blasted to reach saturation (pH = 8.0 ± 0.1, dissolved oxygen > 8.6 mg/l), and different salinities (5‰, 15‰, 25‰, and 35‰) of seawater were artificially filtered. The required concentration used TiO₂ NPs (1 mg/l) and Ag NPs (1 mg/l), and all used suspensions were freshly prepared. Ultrasonic vibration for 30 min was used for the required experiments after the preparation.

2.2 NP Characterization

The particle size distribution of 1 mg/l TiO₂ and Ag NPs dispersed in deionized water and ASW suspensions with different salinities (5‰, 15‰, 25‰, and 35‰) were analyzed using dynamic light scattering (DLS). Ultrasonic vibration for 30 min was immediately conducted after the preparation (all samples were tested for less than 30 min) (Coleman et al., 2011). The time-dependent sedimentation and ion release of TiO₂

and Ag NPs in seawater suspensions with different salinities at 20°C for 24 h were detected by ICP-MS (Liu and Hurt, 2010). The characterization of the two NPs was observed and recorded by field emission scanning electron microscopy (SEM) (Mag = 80.00 kx, EHT = 20.0 kV).

2.3 Holding Conditions and Laboratory Cultures of Study Organisms

M. mongolica

M. mongolica used in this research was initially collected from a marine farm (Zhangzhou). It was then placed in a long-standing stock culture at Xiamen University and consecutively reared for approximately 2 years under controlled laboratory conditions. Briefly, the specimens were maintained in stock culture under semi-static conditions in a 2-l cultivation container filled with 0.22 µm filtered seawater (FSW, salinity 25.0 ± 0.3) at 20 ± 0.5°C and under low light intensity of approximately 400 lx with a 16:8-h light:dark photoperiod in a programmable illuminated incubator (Boxun SPX-2501-G). *M. mongolica* cultures were fed daily with a mixture of two phytoplankton species: 1:1 ratio of *Chlorella vulgaris* and *Isochrysis galbana* in an exponential growth phase at a constant rate of 10⁶ cells/ml. The test used *M. mongolica* stably cultured in a constant temperature light incubator for at least 10 generations in advance according to the conditions required by the experiment, and salinities based on different experimental requirements were 5‰, 15‰, 25‰, and 35‰. These species were fed twice a day, the solution was changed every 2 days, and the newborn individuals were discarded. The fifth-born newborn larvae were used for passage. The larvae used in all experiments were the newborn larvae within 24 h of the 3rd to 5th litter in the domestication group.

2.4 Toxicity Effects of TiO₂ and Ag NPs on *M. mongolica*

Concentrations of TiO₂ and Ag NPs were selected on the basis of preliminary acute and chronic toxicity test results. Initially, a standard acute test method for *Daphnia magna* was used with appropriate modifications based on OECD 211 (OECD, 2012) to determine the toxicity of TiO₂ and Ag NPs to *M. mongolica*.

2.4.1 Acute Toxicity Tests

The tests were set under the conditions of 25‰ salinity and 20 ± 1°C temperature. The test concentrations of TiO₂ NPs are as follows: 1, 2, 3, 4, 5, 6, and 7 mg/l. Meanwhile, the test concentrations of Ag NPs are 0.2, 0.4, 0.6, 0.8, 1.0, and 1.2 mg/l. Each treatment was replicated six times and assigned to a randomized block design. During the first 96 h of the test, each replicate comprised five third-brood neonates (between 6 to 24 h old) that were held in a crystallizing dish (height 5 cm; internal diameter 8.5 cm). A total of 100 ml of test solution was assigned for each concentration group, and six parallel replicates and controls were set. Each replicate group had five healthy and active larvae within 12–24 h of reproduction in three to five fetuses in the acclimation group. The experimental test solution for inhalation was selected in accordance with the low to high

concentrations. After the start of the experiment, observations were made every 6 h, and the dead individuals were sucked out. The identification method of whether the individual died or not was as follows: lightly touch the individual with a dissecting needle and continuously touch them for 18 s to determine the dead individual. The test and control solutions were replaced every 12 h, and the experimental results were recorded accurately for 96 h. The individuals were not fed during the experiment.

2.4.2 Chronic and Generational Survival Toxicity Tests

According to the acute toxicity test and preexperiment results, the exposure groups of five chronic experiments were set under the conditions of 25‰ salinity and 20 ± 1°C temperature, and the concentrations of the TiO₂ NP solution was 0.4, 0.8, 1.6, 3.2, and 6.4 mg/l. The Ag NP solution concentrations were 0.05, 0.1, 0.2, 0.4, 0.8, and 1.6 mg/l. Each concentration group contained 10 ml experimental solution, and 30 parallel replicates and 30 controls were set; each replicate and parallel group was a 20-ml system, and one healthy and active larvae of acclimated groups 3–6 were placed within 24 h of reproduction. The experimental period is 21 days, the experimental solution is replaced every 24 h, and the mixed algal solution is fed once after 12 h of replacement. The solution was fed after shaking and dissolving, and the feeding amount was 3 × 10⁶ cells/l. The survival and larval conditions of the experimental organisms were observed every 12 h and recorded.

According to the results of the 21-day chronic toxicity test experiment, the control group, the two concentration groups of TiO₂ NPs (0.4 and 1.6 mg/l), and the two concentration groups of Ag NPs (0.1 and 0.4 mg/l) were selected for generational exposure experiments. The experimental method aims to select 30 healthy larvae randomly from the third litter of the parent (within 24 h of incubation) as the next generation. Each generation is continuously cultured for 21 days, and the four-generation transmission experiment from F0 to F3 is performed. Other experimental methods and statistical endpoints are the same as those of a 21-day chronic exposure experiment.

2.5 Effect of Salinity on the Toxicity and Bioaccumulation

The salinity is set to the following four gradients: 5‰, 15‰, 25‰, and 35‰. The acute and chronic test methods are the same as those in 2.4 of this study. According to the preexperiment, the initial calibration concentration settings for the acute test of TiO₂ and Ag NPs are as follows: 1, 2, 4, 6 and 0.1, 0.25, 0.5, 1.0 mg/l, respectively; the initial calibration concentration settings of TiO₂ and Ag NP chronic tests are as follows: 1, 2, 4, 6, 8 and 0.05, 0.1, 0.2, 0.4, 0.8, 1.6 mg/l, respectively. The initial individuals of each condition group in the acute experimental group were 10 larvae (within 12–24 h) with three parallels in each group, and the 21-day experimental group with 30 individuals in each group (within 12–24 h) was in parallel.

Cumulative situation: The TiO₂ NPs of 1 and 4 mg/l and the Ag NPs of 0.25 and 1 mg/l exposure groups were selected for the 96-h exposure, and the samples were continuously

sampled every 12 h. Fifty live animals were sampled per batch in each group. NPs accumulate changes and accumulate in larvae before and after molting which were selected from the 2- and 6-mg/l TiO₂ NPs and 0.1- and 0.4-mg/l Ag NP exposure groups for detection of the parent animals and reproductive larvae before and after molt release (and nauplius birth) of one fetus. The specific operations were as follows: when an individual in the same batch had one embryonic molt release (and nauplius birth) in each group, 30 non-reproductive individuals were immediately sampled as samples before molting, 60 non-reproductive individuals were transferred to the same salinity control solution at the same time, and 30 non-reproductive individuals were selected within 6 h. Only individuals were used as post-molt samples, and 50 newly bred larvae were selected as larval samples. Therefore, the accumulated detection samples were dried, weighed, and digested after cleaning, and the corresponding Ti and Ag metal contents were detected by ICP-MS (Agilent-7700x).

2.6 RNA Isolation and Sequencing

Transcriptomic analyses were conducted on six groups of samples; the samples for acute toxicity analysis combined with the experimental results in acute toxicity test were cultured under acute experimental conditions for 60 h (because at this time, both NPs were exposed to significant lethal effects and were in the molting period), and the survival rate of the two NP-exposure conditions was close to 50%. The samples for chronic and reproductive toxicity analysis were selected based on the comprehensive consideration of NP exposure before the third fetus, and each group was selected from the 15th day, and the concentration group with a significant lethal effect and reproductive toxicity is selected. When three reproductive individuals appear in each exposure and control, the fixed non-reproductive individuals serving as samples were immediately selected. Different groups of samples were denoted as Acute-TiO₂ NPs (A-TiO₂), Acute-Ag NPs (A-Ag), Acute-Control (A-0), Chronic-TiO₂ NPs (C-TiO₂), Chronic-Ag NPs (C-Ag), and Chronic-Control (C-0).

The BLASTx program (<http://www.ncbi.nlm.nih.gov/BLAST/>) with an E-value threshold of 1e-5 to the NCBI non-redundant protein (Nr) database (<http://www.ncbi.nlm.nih.gov/>), the Swiss-Prot protein database (<http://www.expasy.ch/sprot>), the Kyoto Encyclopedia of Genes and Genomes (KEGG) database (<http://www.genome.jp/kegg>), and the COG/KOG database (<http://www.ncbi.nlm.nih.gov/COG>) was used to annotate the unigenes. Then, protein functional annotations could be obtained according to the best alignment results.

Each sample was collected and homogenized in TRIzol reagent (Invitrogen, Carlsbad, CA, USA), and RNA was extracted according to the manufacturer's protocol. The use of ethanol precipitation instead of an RNA-binding column in this separation allows us to analyze mRNA and microRNA in one sample. Agarose gel electrophoresis (1.5%), NanoDrop 2000 (Thermo Scientific, Wilmington, USA), and Agilent 2100 Bioanalyzer (Agilent Technologies, Palo Alto, CA, USA)

were used to check the RNA integrity, concentration, and quality. The RNA integrity numbers of the samples were all above 8.0. The same RNA samples were used for mRNA and real-time quantitative PCR (RT-qPCR) analysis.

After the total RNA extracted from each group of samples was qualified, the mRNA was enriched using magnetic beads with Oligo (dT). Fragmentation buffer is then added to break the mRNA into short fragments. The first cDNA strand was synthesized by using a short fragment of mRNA as a template using random hexamers, and then the second cDNA strand was synthesized by adding buffer, dNTPs, RNase H, and DNA polymerase I. After purification by QiaQuick PCR Kit and elution with EB buffer, end repair was performed, poly(A) was added, and sequencing adapters were connected. Then, fragment size selection and recovery were performed by agarose gel electrophoresis, and the recovered products were amplified by PCR. An mRNA library was built. The constructed sequencing library was sequenced with Illumina HiSeq™ 2000.

Gene expression validation refers to the information provided by the supplier; from the RNA samples, 500 ng RNA of each sample was used for reverse transcription to cDNA using a TransScript® AT131 RT Reagent Kit with gDNA Eraser (TaKaRa Biotech Co., Ltd., Dalian, China).

One microliter (50 ng) of each cDNA sample was used for qPCR using the FastStart Universal SYBR Green Master (Roche, Germany) on a LightCycler 96 (Roche, Germany). All reactions were performed in triplicate. All quantifications were performed with beta-actin as a normalized reference, and relative amounts of mRNA were calculated using the 2^{-ΔΔCt} method. Primer specificity was confirmed by evaluating product melting curves. For microRNA RT-qPCR, TransScript Green miRNA Two-Step qRT-PCR SuperMix (TransGen Biotech, Beijing, China) was used to facilitate cDNA synthesis, followed by specific primers for amplification.

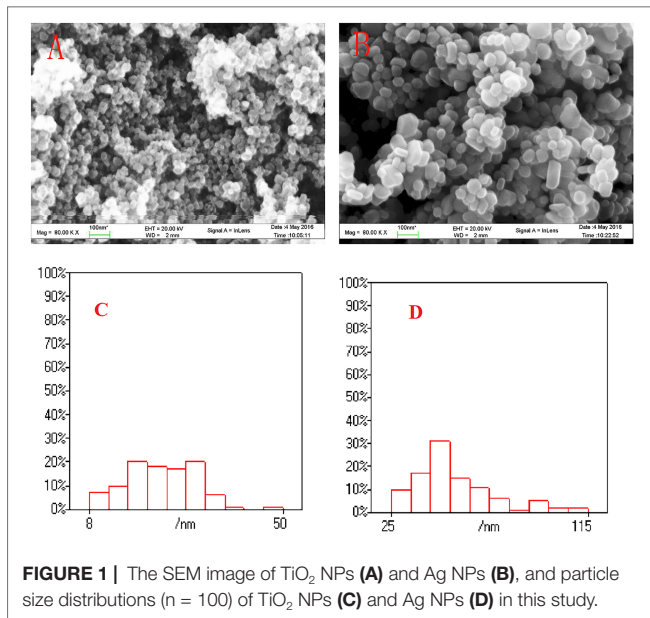
2.7 Statistical Analyses

Acute toxicity tests were performed using SPSS 19.0. All other statistical analyses used R for calculation analysis, and GraphPad Prism was used for graph production. An unpaired t-test was also applied to show statistical differences between negative and positive controls. Significant differences were reported at *P* < 0.05, and results were presented as mean ± standard deviation (S.D.).

3 RESULTS

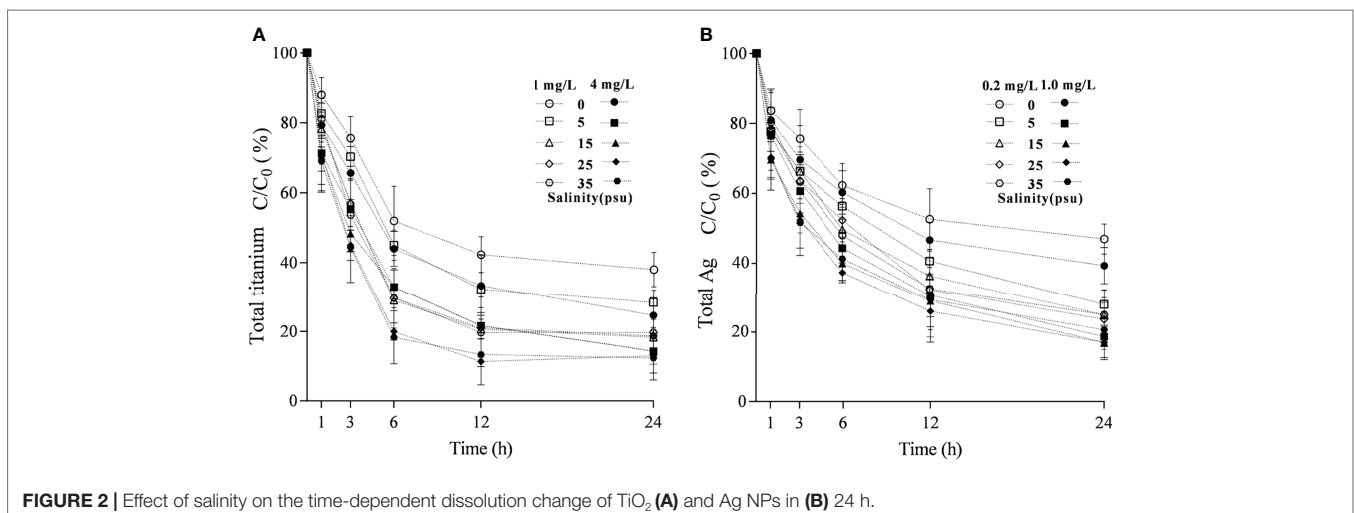
3.1 Characterization of TiO₂ NPs and Ag NPs

The initial SEM and TEM measurements showed the uniform dispersion of the two NPs (**Figure 1A**). The scanning results and particle size analysis revealed that the TiO₂ NPs were approximately spherical particles, while the shape of the Ag NPs was relatively different (regular, spherical, elongated, and irregular) (**Figure 1B**). The particle size range of TiO₂



and Ag NPs is 8.33–49.58 nm (Figure 1C) and 25.00–114 nm (Figure 1D).

The DLS measurements revealed that TiO₂ NP and Ag NP agglomerate and sedimentation are rapidly influenced by high-concentration ions in seawater under laboratory conditions (temperature 20°C and salinity 25). The agglomeration sizes (773.8 and 840.8 nm) of TiO₂ and Ag NPs with average particle sizes of 23.26 and 53.87 nm in seawater with a salinity of 25‰ are substantially larger than those in freshwater (277.6 and 193.14 nm) at nominal values of 1.0 mg/l. The initial dissolution rates of 1.0 mg/l TiO₂ and Ag NPs in fresh water and salinity 25 seawater in 24 h were 38.34%, 18.94% and 39.58%, 17.35%; in four salinity gradients (5‰, 15‰, 25‰, and 35‰), a high salinity leads to the significant settlement of the two NPs. A high initial concentration leads to a low dissolution ratio of the two NPs (Figure 2).



3.2 Effects of Acute and Chronic Exposures to TiO₂ and Ag NPs on *M. mongolica*

The exposure of two NPs at a certain concentration has acute and chronic toxicity effects on *M. mongolica*. The 48-h LC₅₀ and 72-h LC₅₀ of the TiO₂ NP exposure on *M. mongolica* were 10.61 and 4.14 mg/l, respectively, and those of Ag NP exposure were 0.79 and 0.65 mg/l, respectively (Table 1). The 21-day chronic experiment showed that the exposure time and concentration of the two NPs had significant effects on the mortality rate ($P < 0.05$) (Figure S1). However, only the highest-concentration group (6.4 mg/l) of TiO₂ NP exposure had a significant negative impact on the reproduction and intrinsic rate of population increase (r_m) of *M. mongolica*. All the TiO₂ NP exposure groups did not induce aborted offspring. Ag NP exposure showed toxicity not only on the mortality rate but also on reproduction and generations. The concentration of Ag NP exposure above 0.2 mg/l reduced reproduction and decreased the number of offspring and r_m , and the increase in the number of abortions was significantly different from the control group (Figure 3). The experiment over three generations showed no significant difference in the survival between the control group and the TiO₂ NP exposure groups but significantly affected the Ag NP exposure of *M. mongolica*. The survival rate of the Ag NP exposure group decreased with three generations of Ag NP exposure. Therefore, Ag NPs may be highly genotoxic to *M. mongolica*.

The experiment revealed that the two NP aggregates were filled inside the digestive tracts and molt carapace (Figure 4).

3.3 Effect of Salinity on the Toxicity and Bioaccumulation of NPs

This study analyzed the effects of salinity changes on the acute exposure and toxicity of two NPs. The results showed that acute and chronic toxicity exposure of the two NPs was significantly affected by salinity changes (Figures S2, 3), but the trends of toxicity effect were opposite with the exposure of the two

TABLE 1 | Comparison of effect concentrations of TiO₂ and Ag NPs on *M. mongolica* after acute exposure.

NPs		LC10 (CI) (mg/L)	LC50 (CI) (mg/L)	df	R ²	Sy.x
TiO ₂	48 h	17.10 (11.34–22.86)	10.61 (2.63–18.58)	47	0.43	1.76
	72 h	6.33 (5.67–7.00)	4.14 (3.15–5.13)	47	0.81	1.04
Ag	48 h	1.12 (0.94–1.29)	0.79 (0.55–1.03)	41	0.68	0.23
	72 h	1.03 (0.94–1.11)	0.65 (0.52–0.78)	41	0.89	0.14

NPs. The increase in salinity enhanced the toxicity of TiO₂ NP exposure to *M. mongolica*, while the toxicity of Ag NP exposure was decreased.

The largest difference in reproductive effects caused by TiO₂ and Ag NP exposure was reflected in the death of reproductive larvae. Neither the control group nor the TiO₂ NP exposure groups under all salinity conditions resulted in the death of reproductive larvae. However, in the Ag NP exposure groups, the larval death phenomenon occurred at all salinities and exposures at different concentrations (Figure 5). In the medium- and low-concentration Ag NP exposure groups (≤ 0.4 mg/l), the death rate of reproductive larvae of *M. mongolica* increased with the decrease in salinity, and the high-concentration group did not demonstrate effective accumulation for 21 days in the salinity below 15‰ larvae. The comparison between the conditions of 25‰ and 35‰ revealed that the cumulative death rate of the larvae in the 35‰ condition was higher than that in the 25‰ salinity exposure group when the Ag NP exposure concentration was larger than or equal to 0.8 mg/l.

The salinity changes also significantly affected the bioaccumulation of *M. mongolica*. The effect of salinity on the accumulation of two NPs is different. The accumulation of TiO₂ NPs was the highest when the salinity is 15‰, while that of Ag NPs was the highest at 5‰ and then decreased significantly with the increase in salinity. The results also revealed that the NPs that accumulated on the carapace (between before and after molting) of the two NPs were the main accumulation modes (approximately 40%–60% of all accumulations), which increased with salinity. The nauplius test from adult exposure in the two NPs showed that the Ag accumulation of Ag NP exposure was higher than that of TiO₂ NP exposure, which was consistent

with the high mortality rate of nauplius from Ag NP exposure in adults (Figure 6).

3.4 Transcriptome Analysis

3.4.1 Sequence Assembly and Generation

After trimming and quality assessment, each group's approximated 47,602,732–71,049,522 clean reads were obtained for all samples (Table S1). Eighty-seven percent of these clean reads were successfully aligned to the reference genome. For *de novo* assembly and transcription-level comparative analysis, we successfully constructed the *M. mongolica* mRNA library and obtained high-quality transcription information. A total of 27,274 genes were assembled, and 11,056 genes were successfully compared with the four databases. All the annotated genes had the highest homology with *Daphnia magna*.

To explore the overall differences between the *M. mongolica* expression profiles at different exposure conditions (A-TiO₂, A-Ag, A-0, C-TiO₂, C-Ag, and C-0), all unigenes were used for principal component analysis (PCA), and the result showed that the biological replicates of each time point were close to each other and far from the other time points (Figure S4). Fourteen genes with significant differences, such as antioxidant, detoxification, case and digestion, were selected for RT-qPCR (Table S2). Identical results were acquired to RNA-Seq findings, verifying the reproducibility and reliability of the RNA-Seq data. The information of all differential genes is displayed in Supplementary Data S1.

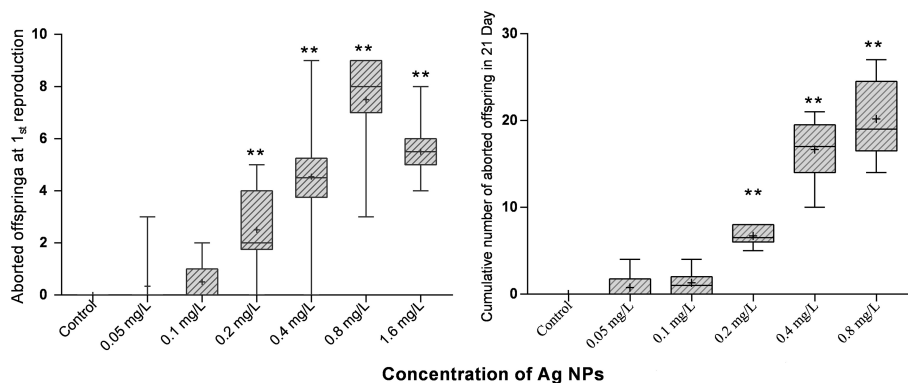


FIGURE 3 | *M. mongolica* abdomen abortion due to exposure to Ag NPs. **Indicates values that are significantly different between different Ag NPs treatments groups ($P < 0.05$).

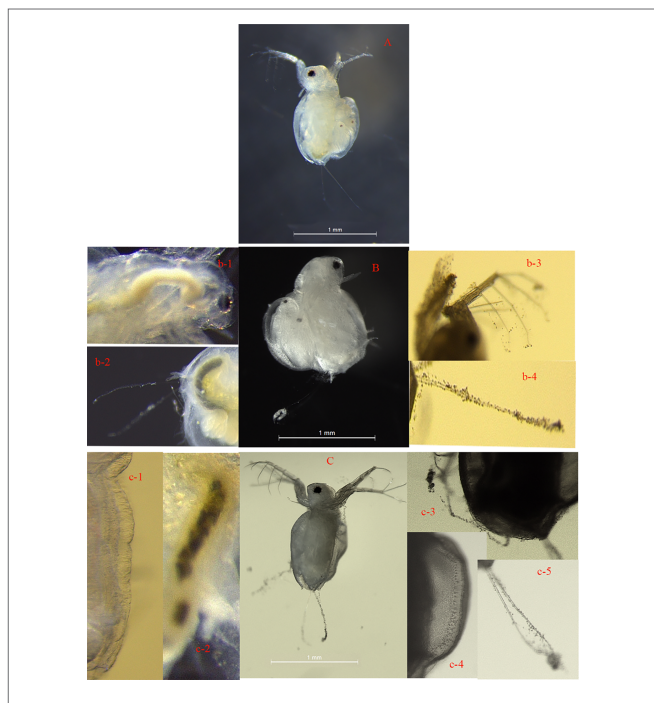


FIGURE 4 | Visual images of *M. mongolica* after 15 days of chronic exposure to control solution (A), 3.2 mg/l TiO₂ NPs (B), 0.8 mg/l Ag NPs (C). TiO₂ NPs accumulated inside the digestive tract (b-1, and b-2). TiO₂ NPs heavily adsorbed on the carapace and distributed over the antennae, carapace, and apical spine (b-3 and b-4) of the *M. mongolica* body. Ag NPs adsorbed on the carapace, and the carapace (c-1, c-3, and c-4) accumulated inside the digestive tract (c-2) and distributed over the antennae (c-5) of the *M. mongolica* body. Exposure to Ag NPs, no egg laying of *M. mongolica*.

3.4.2 GO and KEGG Pathway Enrichment Analysis of Differentially Expressed Genes

The reads obtained were used in the downstream analyses to

compare acute and chronic experimental samples with the controls to quantitatively evaluate the inhibition or increase in gene expression. The numbers of differentially expressed genes (DEGs) in *M. mongolica* exposed to acute and chronic NP exposure tests with respect to controls are shown in **Figure S5**. Between acute exposure groups, there were a total of 667 DEGs (297 up-regulated, 370 down-regulated) in A-TiO₂ groups and 266 DEGs (106 up-regulated, 160 down-regulated) in A-Ag between controls. Between chronic exposure groups, C-TiO₂ groups collected 619 DEGs (344 up-regulated, 275 down-regulated), and C-Ag groups collected 198 DEGs (129 up-regulated, 69 down-regulated) between controls (**Table S3**).

To understand the distribution of DEGs at a macro level, the DEGs were mapped in accordance with the GO terms and the KEGG pathway (**Supplementary Data S2**), respectively. The results demonstrated that these DEGs were involved in the biological process of single organism, cellular, metabolic, locomotion, development, immune system, etc., with molecular function of binding catalytic and transporter activity (**Figure 7**). In addition, A-TiO₂ and C-TiO₂ groups were highly related to localization.

For better clarifying those biological pathways related to NP exposure, KEGG pathway enrichment analysis was also used to further elucidate the putative functions of these DEGs; the top 20 pathways are exhibited in **Figure 8**. KEGG pathway enrichment analysis demonstrated that most up-regulated DEGs in A-TiO₂ groups were widely related with cuticles (e.g., amino sugar and nucleotide sugar metabolism, mucin type O-glycan biosynthesis pathway) and signaling pathways (e.g., neuroactive ligand–receptor interaction and ECM–receptor interaction). In addition, immune responses (e.g., lysosome and peroxisome) and oxidative stress (e.g., glutathione metabolism and peroxisome) were found to be the most-enriched pathways in down-regulated DEGs (**Figure 8A**). Up-regulated genes in

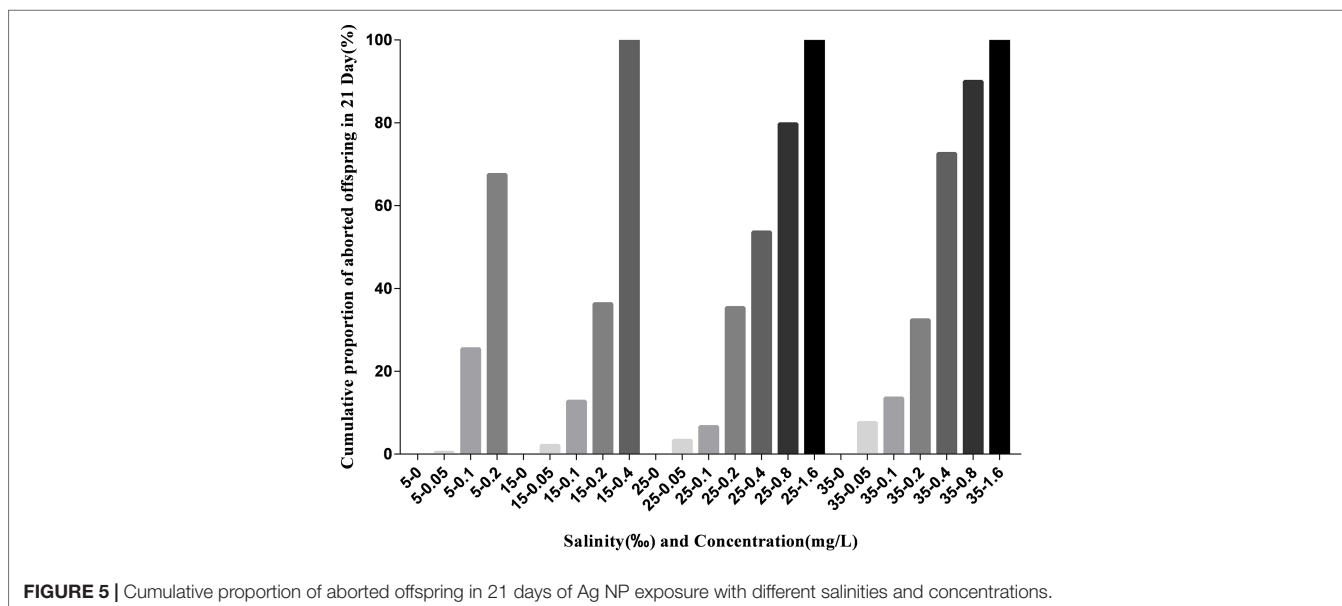
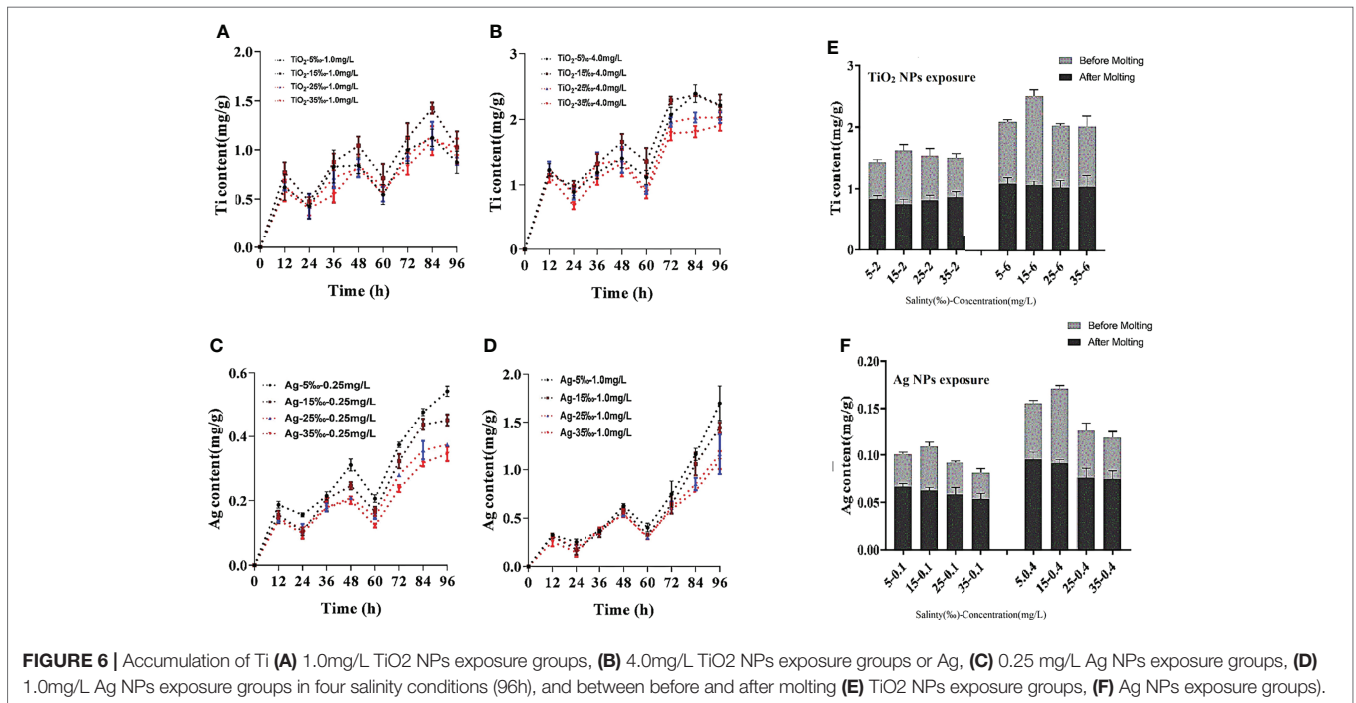
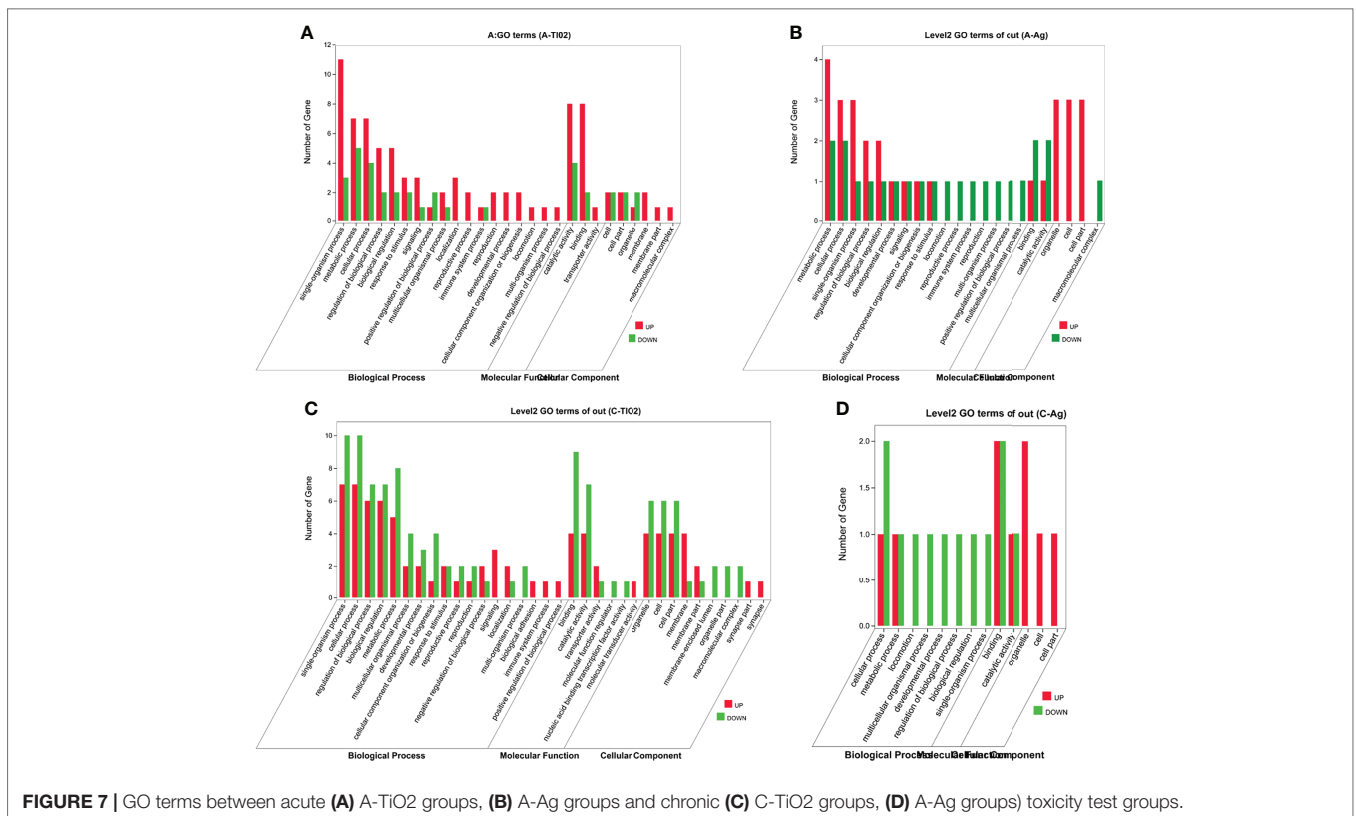


FIGURE 5 | Cumulative proportion of aborted offspring in 21 days of Ag NP exposure with different salinities and concentrations.



A-Ag groups were highly related to ABC transporters, immune responses, etc.; down-regulated DEGs were related to cuticle, oxidative stress, metal detoxification (cytochrome P450), and apoptosis pathway (Figure 8B). C-TiO₂ groups were widely

related with cuticle and immune responses in up-regulated DEGs, and reproduction and growth regulation in down-regulated DEGs (Figure 8C). C-Ag groups were widely related with metal detoxification, transmembrane transport, and



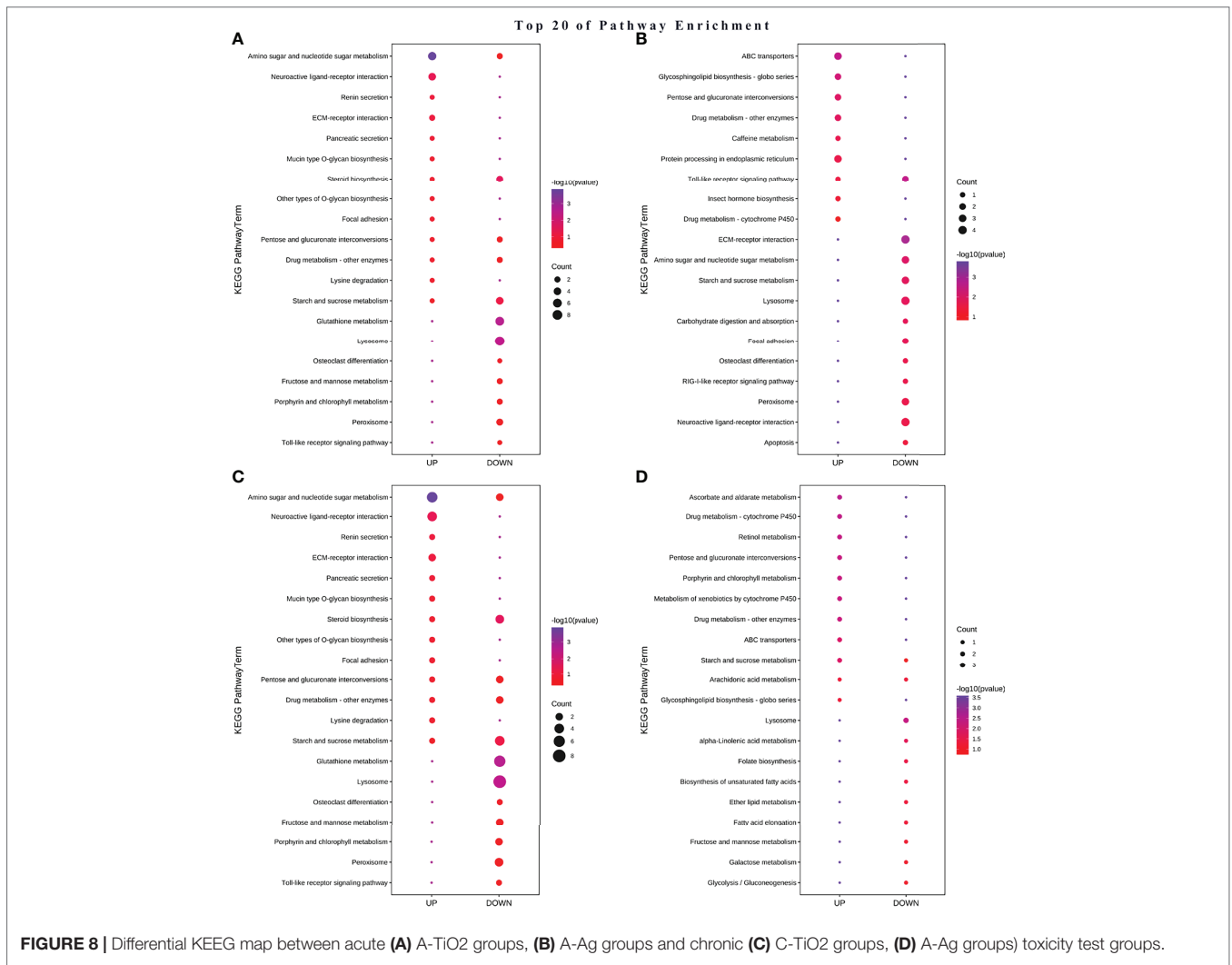
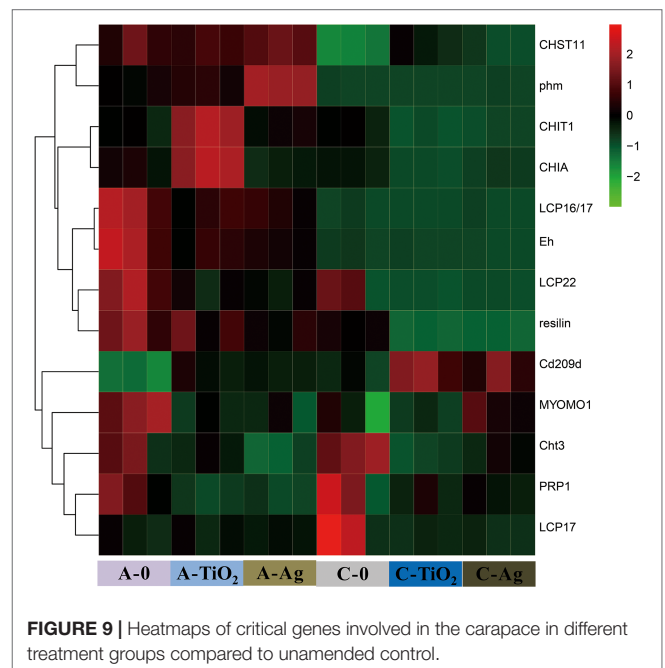


FIGURE 8 | Differential KEGG map between acute (A) A-TiO₂ groups, (B) A-Ag groups and chronic (C) C-TiO₂ groups, (D) A-Ag groups) toxicity test groups.

immune responses in up-regulated DEGs, lysosome, energy metabolism (e.g., arachidonic acid metabolism and starch and sucrose metabolism), and growth regulation in down-regulated DEGs (Figure 8D). Moreover, A-TiO₂ and C-TiO₂ groups were observed in renin secretion up-regulated pathways different from A-Ag and C-Ag groups. Conversely, metal detoxification-related DEGs, such as cytochrome P450, pentose and glucuronate interconversions, and ascorbate and aldarate metabolism pathways, were observed in A-Ag and C-Ag groups (Châtel and Mouneyrac, 2017; Huang et al., 2020).

3.5 Critical DEGs Involved in Carapace in *M. mongolica*

GO and KEGG pathway enrichment analyses showed that the DEGs in all NP-treated groups were highly related to the cuticle, which is the main component of the carapace. To further understand the mechanism of the carapace related with *M. mongolica*, we identified a few key DEGs that might be related to the carapace; these DEPs in NP-treated groups were mainly grouped into the following functions: related to carapace (PRP1, LCP17, LCP22, LCP16/17, MYOMOD1,



and resilin), related to chitin (CHIT1, CHIA, Cht3, CHST11) and ecdysone (p_{hm} and Eh), and related to growth (Cd209d) (Figure 9).

4 DISCUSSION

4.1 Toxicity Comparison of TiO₂ and Ag NP Exposure to *M. mongolica*

Acute, chronic, reproductive, and generational experiments in this study showed that Ag NPs had stronger toxicity and faster toxic effects than TiO₂ NPs. Particularly, Ag NPs showed strong reproductive and generational toxicity, while TiO₂ NPs were insignificant. This result is in agreement with that of many previous studies, in which Ag NPs are highly toxic to aquatic organisms (Griffitt et al., 2008; Arulvasu et al., 2014; Orbea et al., 2017), while TiO₂ NPs had low toxicity (Adams et al., 2006; Wiesenthal et al., 2011; Amiano et al., 2012; Hartmann et al., 2012; Ates et al., 2013; Lu et al., 2018). This finding is related to the two toxic mechanisms of NPs: particle toxicity and release of metal ions.

Ag⁺ released by Ag NPs has metal toxicity and can quickly enter the body and with seawater, which might be responsible for strong reproductive toxicity and larval mortality. In seawater, Ag will be converted into AgCl_{0(aq)} with high bioavailability (Engel et al., 1981). Thus, Ag NP exposure to *M. mongolica* facilitates absorption and utilization, thereby rapidly producing strong toxicity. Arulvasu et al. found that Ag NPs had toxic effects on the survival, molting, hatching rate, and generation of *Artemia* (Arulvasu et al., 2014), and Ag NPs could cause malformations in zebrafish embryos (Orbea et al., 2017) similar to the results of this study.

Data of GO and KEGG showed that metal detoxification and reproductive repair were severely impacted in A-Ag as well as C-Ag groups, and down-regulated genes showed that oxidative stress, immune stress, and detoxification were inhibited. These results were considered to be related to Ag⁺ toxicity in previous studies (Eom and Choi, 2010; Fabrega et al., 2011; Piao et al., 2011) and different between the TiO₂ NP exposure group in this study. Further analysis showed that the total number of DEGs was several times less than in the TiO₂ NP exposure group; this phenomenon was similar to the comparison of Ag NP and AgNO₃ exposure results, but the number of DEGs of AgNO₃ exposure was smaller (Piersanti et al., 2021). Moreover, pathway enrichment was related to apoptosis in A-Ag and C-Ag. These results were triggered by Ag NP-released Ag⁺ ions.

4.2 Salinity-Based Toxicity of TiO₂ and Ag NPs to *M. mongolica*

NPs will agglomerate in seawater, and the sizes of TiO₂ and Ag NP aggregates all increased with salinity in this study. Both NPs released metal ions in seawater, but their ion release showed the opposite (Figure 2). The release of Ti⁴⁺ from TiO₂ NPs in seawater was lower than that in freshwater and decreased with increasing salinity. Meanwhile, the Ag⁺ released from Ag NPs increased with salinity. Moreover, salinity affects the accumulation and

accumulation on the carapace of the two NPs in *M. mongolica*. Under high salinity, the total accumulation of Ti is high, while that of Ag is low (Figure 7). This finding may also affect the toxicity of the two NPs under different salinity conditions.

The toxicity of TiO₂ NPs to *M. mongolica* increased with salinity, but opposite results were observed for Ag NPs. This finding may be related to the influence of salinity on the dissolution and the different toxicity mechanisms of the two NPs. TiO₂ NPs mainly have particle toxicity and suggest carapace damage to *M. mongolica*, while Ag NPs also have toxicity by release of Ag⁺. The agglomeration of TiO₂ NPs was enhanced with the increase in salinity, and the accumulation and adhesion on the carapace leading to toxicity were enhanced. Meanwhile, the agglomeration of Ag NPs was also enhanced, but Ag⁺ was bound by high concentrations of Cl⁻, which reduced the Ag⁺ metal toxicity. At high salinity, the dominant species of inorganic Ag shifts to negatively charged silver (i.e., AgCl²⁻, AgCl₃²⁻) which is less bioavailable than AgCl_{0(aq)} (Chan and Chiu, 2015). Previous studies have also shown that the toxicity of ZnO-NPs to the marine diatom decreased with increasing salinity (Chan and Chiu, 2015). In addition, salinity changes also affect the osmotic pressure of the organism, and TiO₂ NP-treated groups resulted in up-regulated DEGs of renin secretion in this study. Accordingly, salinity also affects the osmotic regulation of organism exposure to NPs.

Salinity factor affects various mechanisms such as NP aggregation, ion release, and ion bioavailability and osmotic pressure sensitivity of organisms, thereby affecting the toxicity of NPs in seawater (Keller et al., 2010). Therefore, salinity factors are key to designing and interpreting nanoparticle ecotoxicity studies in marine areas.

4.3 Carapace Damage May Be One of the Main Toxic Mechanisms of the Two NPs to *M. mongolica*

Both two NP aggregates and adhesion on carapace (Figure 4) and the cumulative ratio of the carapace were remarkably high (approximately 40%–60%, Figure 8). The phenomenon of NPs adhering to the surface of aquatic organisms, such as *Daphnia magna*, *Artemia*, *Nereid*, and *marine medaka*, has been found in many studies (Allen et al., 2010; Zuykov et al., 2011; Al-Sid-Cheikh et al., 2013).

This finding shows that two NP responses suggest that carapace damage influences the defense, growth, molting, and reproduction of *M. mongolica*. Transcriptional analysis was consistent with this conclusion. GO and pathway enrichment analyses of DEGs in all NP-treated groups showed critical DEGs involved in carapace in *M. mongolica* (Figure 9). The carapace of cladocerans is associated with defense, growth, reproduction, and molting (Repka et al., 1995; Jia et al., 2018). Particularly in the two NP exposure groups, the following were observed: high mortality rates before and after the molt release (and nauplius birth), carapace damage, and molting difficulties caused by the adhesion of NPs on *M. mongolica* carapace and the possible fragility of *M. mongolica* at this stage.

Interestingly, the influence of simulated microgravity of *Daphnia magna* affected the pathway of pentose phosphate and fructose and mannose metabolism (Trotter et al., 2015); these pathways were also affected in the NP treatment groups, and due to NP aggregates and adhesion on the carapace, *M. mongolica* may also be affected by the stressful condition of altered gravity. In addition, salinity also affected two NP aggregates on the carapace of *M. mongolica*. Carapace damage may be one of the main toxic mechanisms of the two NPs in seawater.

5 CONCLUSION

This study combined ecotoxicology, transcriptomics, and the effects of salinity factors to analyze the toxic effects of TiO₂ and Ag NPs on *M. mongolica*. The toxicity sources of metal and metal oxide NPs in seawater include special NP particle toxicity and metal ion toxicity. TiO₂ and Ag NPs have NP particle toxicity effects on *M. mongolica*, which would cause oxidative and immune stresses, respectively. One of the main toxic mechanisms is carapace damage due to aggregate adhesion of two NPs. Ag NPs have stronger acute, chronic, and reproductive toxicity mainly due to the metal toxicity caused by the release of Ag⁺. In seawater, the salinity factor affects various aspects, including the dissolution of NPs and different toxicity mechanisms. Comprehensively considering the conditions of the test organisms and NPs is necessary to assess the toxicity of NPs in seawater.

DATA AVAILABILITY STATEMENT

The sequence files of RNAseq data presented in the study are deposited in the GenBank repository, accession number PRJNA824670.

REFERENCES

- Adams, L. K., Lyon, D. Y., McIntosh, A. and Alvarez, P. J. J. (2006). Comparative Toxicity of Nano-Scale TiO₂, SiO₂ and ZnO Water Suspensions. *Water Sci. Technol.* 54 (11-12), 327–334. doi: 10.2166/wst.2006.891
- Adam, N., Vergauwen, L., Blust, R. and Knäpen, D. (2015). Gene Transcription Patterns and Energy Reserves in *Daphnia magna* Show No Nanoparticle Specific Toxicity When Exposed to ZnO and CuO Nanoparticles. *Environ. Res.* 138, 82–92. doi: 10.1016/j.envres.2015.02.014
- Allen, H. J., Impellitteri, C. A., Macke, D. A., Heckman, J. L., Poynton, H. C., Lazorchak, J. M., et al. (2010). Effects From Filtration, Capping Agents, and Presence/Absence of Food on the Toxicity of Silver Nanoparticles to *Daphnia magna*. *Environ. Toxicol. Chem.* 29 (12), 2742–2750. doi: 10.1002/etc.329
- Al-Sid-Cheikh, M., Rouleau, C. and Pelletier, E. (2013). Tissue Distribution and Kinetics of Dissolved and Nanoparticulate Silver in *Iceland Scallop (Chlamys Islandica)*. *Mar. Environ. Res.* 86, 21–28. doi: 10.1016/j.marenvres.2013.02.003
- Amiano, I., Olabarrieta, J., Vitorica, J. and Zorita, S. (2012). Acute Toxicity of Nanosized TiO₂ to *Daphnia magna* Under UVA Irradiation. *Environ. Toxicol. Chem.* 31 (11), 2564–2566. doi: 10.1002/etc.1981
- Arulvasu, C., Jennifer, S. M., Prabhu, D. and Chandhirasekar, D. (2014). Toxicity Effect of Silver Nanoparticles in Brine *Shrimp Artemia*. *Sci. World J.* 2014, 256919–256919. doi: 10.1155/2014/256919
- Asharani, P. V., Wu, Y. L., Gong, Z. and Valiyaveetil, S. (2008). Toxicity of Silver Nanoparticles in Zebrafish Models. *Nanotechnology* 19 (25), 255102. doi: 10.1088/0957-4484/19/25/255102
- Ates, M., Daniels, J., Arslan, Z. and Farah, I. O. (2013). Effects of Aqueous Suspensions of Titanium Dioxide Nanoparticles on *Artemia salina*: Assessment of Nanoparticle Aggregation, Accumulation, and Toxicity. *Environ. Monit. Assess.* 185 (4), 3339–3348. doi: 10.1007/s10661-012-2794-7

AUTHOR CONTRIBUTIONS

JH sorted the data. JH and YL wrote the original draft. JH completed the experiment. YL and SL performed the investigation and provided advice. YL provided funding. All authors contributed to the article and approved the submitted version.

FUNDING

This study was supported by the National Natural Science Foundation of China (Grant No. U1805241) and National Marine Public Welfare Project of China (201505034).

ACKNOWLEDGMENTS

Special thanks are given to Professor Wenqing Cao from the College of Ocean and Earth Sciences, Xiamen University, for her support and help; she was one of the earliest researchers to study *M. mongolica*, and this research is only to commemorate her. The authors gratefully thank Zhipeng Li (College of Ocean Food and Biology Engineering, Jimei University, Xiamen, China) for his assistance in transcriptome analysis.

SUPPLEMENTARY MATERIAL

The Supplementary Material for this article can be found online at: <https://www.frontiersin.org/articles/10.3389/fmars.2022.909701/full#supplementary-material>

- Auffan, M., Rose, J., Wiesner, M. R. and Bottero, J. Y. (2009). Chemical Stability of Metallic Nanoparticles: A Parameter Controlling Their Potential Cellular Toxicity *In Vitro*. *Environ. pollut.* 157 (4), 1127–1133. doi: 10.1016/j.envpol.2008.10.002
- Brunelli, A., Pojana, G., Callegaro, S. and Marcomini, A. (2013). Agglomeration and Sedimentation of Titanium Dioxide Nanoparticles (N-TiO₂) in Synthetic and Real Waters. *J. Nanoparticle Res.* 15 (6)1684. doi: 10.1007/s11051-013-1684-4
- Chan, C. Y. S. and Chiu, J. M. Y. (2015). Chronic Effects of Coated Silver Nanoparticles on Marine Invertebrate Larvae: A Proof of Concept Study. *PLoS One* 10 (7), e0132457. doi: 10.1371/journal.pone.0132457
- Châtel, A. and Mouneyrac, C. (2017). Signaling Pathways Involved in Metal-Based Nanomaterial Toxicity Towards Aquatic Organisms. *Comp. Biochem. Physiol. Part C: Toxicol. Pharmacol.* 196, 61–70. doi: 10.1016/j.cbpc.2017.03.014
- Clément, L., Hurel, C. and Marmier, N. (2013). Toxicity of TiO₂ Nanoparticles to Cladocerans, Algae, Rotifers and Plants – Effects of Size and Crystalline Structure. *Chemosphere* 90 (3), 1083–1090. doi: 10.1016/j.chemosphere.2012.09.013
- Coleman, V. A., Jänting, Å.K. and Roy, M. (2011). Nanoparticles and Metrology: A Comparison of Methods for the Determination of Particle Size Distributions. *Proc. Spie* 8105 (4), 461–510. doi: 10.1117/12.894297
- Corsi, I., Bergami, E. and Grassi, G. (2020). Behavior and Bio-Interactions of Anthropogenic Particles in Marine Environment for a More Realistic Ecological Risk Assessment. *Front. Environ. Sci.* 8. doi: 10.3389/fenvs.2020.00060
- Corsi, I., Cherr, G. N., Lenihan, H. S., Labille, J., Hasselov, M., Canesi, L., et al. (2014). Common Strategies and Technologies for the Ecosafety Assessment and Design of Nanomaterials Entering the Marine Environment. *ACS Nano* 8 (10), 9694–9709. doi: 10.1021/nn504684k
- Davarazar, M., Kamali, M. and Lopes, I. (2021). Engineered Nanomaterials for (Waste)Water Treatment - A Scientometric Assessment and Sustainability Aspects. *NanoImpact* 22, 100316. doi: 10.1016/j.nimpact.2021.100316

- Du, X., Zhou, W., Zhang, W., Sun, S., Han, Y., Tang, Y., et al. (2021). Toxicities of Three Metal Oxide Nanoparticles to a Marine Microalga: Impacts on the Motility and Potential Affecting Mechanisms. *Environ. pollut.* 290, 118027. doi: 10.1016/j.envpol.2021.118027
- Engel, D. W., Sunda, W. G. and Fowler, B. A. (1981). *Biological Monitoring of Marine Pollution*. Eds. Vernberg, W. B., Thurberg, F. P., Calabrese, A. and Vernberg, F. J. (New York: Academic Press), pp 127–pp 144.
- Eom, H.-J. and Choi, J. (2010). P38 MAPK Activation, DNA Damage, Cell Cycle Arrest and Apoptosis as Mechanisms of Toxicity of Silver Nanoparticles in Jurkat T Cells. *Environ. Sci. Technol.* 44 (21), 8337–8342. doi: 10.1021/es1020668
- Fabrega, J., Luoma, S. N., Tyler, C. R., Galloway, T. S. and Lead, J. R. (2011). Silver Nanoparticles: Behaviour and Effects in the Aquatic Environment. *Environ. Int.* 37 (2), 517–531. doi: 10.1016/j.envint.2010.10.012
- Fajardo, C., Martínez-Rodríguez, G., Blasco, J., Mancera, J. M., Thomas, B. and De Donato, M. (2022). Nanotechnology in Aquaculture: Applications, Perspectives and Regulatory Challenges. *Aquacult. Fish.* 7 (2), 185–200. doi: 10.1016/j.aaf.2021.12.006
- Gagné, F., André, C., Skirrow, R., Gélinas, M., Auclair, J., van Aggelen, G., et al. (2012). Toxicity of Silver Nanoparticles to Rainbow Trout: A Toxicogenomic Approach. *Chemosphere* 89 (5), 615–622. doi: 10.1016/j.chemosphere.2012.05.063
- Gong, N., Shao, K., Li, G. and Sun, Y. (2016). Acute and Chronic Toxicity of Nickel Oxide Nanoparticles to *Daphnia Magna*: The Influence of Algal Enrichment. *NanoImpact* 3-4, 104–109. doi: 10.1016/j.impact.2016.08.003
- Griffitt, R. J., Lavelle, C. M., Kane, A. S., Denslow, N. D. and Barber, D. S. (2013). Chronic Nanoparticulate Silver Exposure Results in Tissue Accumulation and Transcriptomic Changes in Zebrafish. *Aquat. Toxicol.* 130-131, 192–200. doi: 10.1016/j.aquatox.2013.01.010
- Griffitt, R. J., Luo, J., Gao, J., Bonzongo, J. C. and Barber, D. S. (2008). Effects of Particle Composition and Species on Toxicity of Metallic Nanomaterials in Aquatic Organisms. *Environ. Toxicol. Chem.* 27 (9), 1972–1978. doi: 10.1897/08-002.1
- Hartmann, N. B., Legros, S., Kammer, F. V. D., Hofmann, T. and Baun, A. (2012). The Potential of TiO₂ Nanoparticles as Carriers for Cadmium Uptake in Lumbriculus Variegatus and *Daphnia Magna*. *Aquat. Toxicol.* 118–119 (2), 1–8. doi: 10.1016/j.aquatox.2012.03.008
- He, Z. H., Qin, J. G., Wang, Y., Jiang, H. and Wen, Z. (2001). Biology of *Moina Mongolica* (Moinidae, Cladocera) and Perspective as Live Food for Marine Fish Larvae: Review. *Hydrobiologia* 457 (1), 25–37. doi: 10.1023/A:1012277328391
- Huang, M., Keller, A. A., Wang, X., Tian, L., Wu, B., Ji, R., et al. (2020). Low Concentrations of Silver Nanoparticles and Silver Ions Perturb the Antioxidant Defense System and Nitrogen Metabolism in N₂-Fixing Cyanobacteria. *Environ. Sci. Technol.* 54 (24), 15996–16005. doi: 10.1021/acs.est.0c05300
- Ivask, A., Elbadawy, A., Kaweeteerawat, C., Boren, D., Fischer, H., Ji, Z., et al. (2014). Toxicity Mechanisms in *Escherichia Coli* Vary for Silver Nanoparticles and Differ From Ionic Silver. *ACS Nano* 8 (1), 374–386. doi: 10.1021/nn4044047
- Jia, J., Liu, X., Li, L., Lei, C., Dong, Y., Wu, G., et al. (2018). Transcriptional and Translational Relationship in Environmental Stress: RNAseq and ITRAQ Proteomic Analysis Between Sexually Reproducing and Parthenogenetic Females in *Moina Micrura*. *Front. Physiol.* 9. doi: 10.3389/fphys.2018.00812
- Kang, J. S., Bong, J., Choi, J.-S., Henry, T. B. and Park, J.-W. (2016). Differentially Transcriptional Regulation on Cell Cycle Pathway by Silver Nanoparticles From Ionic Silver in Larval Zebrafish (*Danio Rerio*). *Biochem. Biophys. Res. Commun.* 479 (4), 753–758. doi: 10.1016/j.bbrc.2016.09.139
- Keller, A. A., Wang, H., Zhou, D., Lenihan, H. S., Cherr, G., Cardinale, B. J., et al. (2010). Stability and Aggregation of Metal Oxide Nanoparticles in Natural Aqueous Matrices. *Environ. Sci. Technol.* 44 (6), 1962–1967. doi: 10.1021/es902987d
- Khosravi-Katuli, K., Prato, E., Lofrano, G., Guida, M. and Libralato, G. (2017). Effects of Nanoparticles in Species of Aquaculture Interest. *Environ. Sci. pollut. Res.* 24 (11). doi: 10.1007/s11356-017-9360-3
- Liu, J. and Hurt, R. H. (2010). Ion Release Kinetics and Particle Persistence in Aqueous Nano-Silver Colloids. *Environ. Sci. Technol.* 44 (6), 2169–2175. doi: 10.1021/es9035557
- Liu, A., Zhang, M., Kong, L., Wu, D., Weng, X., Wang, D., et al. (2014). Cloning and Expression Profiling of a Cuticular Protein Gene in *Daphnia Carinata*. *Dev. Genes Evol.* 224 (3), 129–135. doi: 10.1007/s00427-014-0469-9
- Lu, J., Tian, S., Lv, X., Chen, Z., Chen, B., Zhu, X., et al. (2018). TiO₂ Nanoparticles in the Marine Environment: Impact on the Toxicity of Phenanthrene and Cd²⁺ to Marine Zooplankton *Artemia Salina*. *Sci. Total Environ.* 615, 375–380. doi: 10.1016/j.scitotenv.2017.09.292
- Magesky, A., Ribeiro, C. A. O. and Pelletier, É. (2016). Physiological Effects and Cellular Responses of Metamorphic Larvae and Juveniles of Sea Urchin Exposed to Ionic and Nanoparticulate Silver. *Aquat. Toxicol.* 174, 208–227. doi: 10.1016/j.aquatox.2016.02.018
- Matranga, V. and Corsi, I. (2012). Toxic Effects of Engineered Nanoparticles in the Marine Environment: Model Organisms and Molecular Approaches. *Mar. Environ. Res.* 76, 32–40. doi: 10.1016/j.marenvres.2012.01.006
- Minetto, D., Libralato, G. and Volpi Ghirardini, A. (2014). Ecotoxicity of Engineered TiO₂ Nanoparticles to Saltwater Organisms: An Overview. *Environ. Int.* 66, 18–27. doi: 10.1016/j.envint.2014.01.012
- OECD (2004). “Test No. 202: *Daphnia* Sp. Acute Immobilisation Test,” in *OECD Guidelines for the Testing of Chemicals, Section 2 Paris* (OECD Publishing). doi: 10.1787/9789264069947-en
- OECD (2012). “Test No. 211: *Daphnia Magna* Reproduction Test,” in *OECD Guidelines for the Testing of Chemicals, Section 2* (Paris: OECD Publishing). doi: 10.1787/20745761
- Orbea, A., González-Soto, N., Lacave, J. M., Barrio, I. and Cajaraville, M. P. (2017). Developmental and Reproductive Toxicity of PVP/PEI-Coated Silver Nanoparticles to Zebrafish. *Comp. Biochem. Physiol. Part C: Toxicol. Pharmacol.* 199, 59–68. doi: 10.1016/j.cbpc.2017.03.004
- Pan, Y., Zhang, W. and Lin, S. (2018). Transcriptomic and Micronaomic Profiling Reveals Molecular Mechanisms to Cope With Silver Nanoparticle Exposure in the Ciliate *Euplotes Vannus*. *Environ. Science: Nano* 5 (12), 2921–2935. doi: 10.1039/C8EN00924D
- Paterson, G., Ataria, J. M., Hoque, M. E., Burns, D. C. and Metcalfe, C. D. (2011). The Toxicity of Titanium Dioxide Nanopowder to Early Life Stages of the Japanese Medaka (*Oryzias Latipes*). *Chemosphere* 82 (7), 1002–1009. doi: 10.1016/j.chemosphere.2010.10.068
- Piao, M. J., Kang, K. A., Lee, I. K., Kim, H. S., Kim, S., Choi, J. Y., et al. (2011). Silver Nanoparticles Induce Oxidative Cell Damage in Human Liver Cells Through Inhibition of Reduced Glutathione and Induction of Mitochondria-Involved Apoptosis. *Toxicol. Lett.* 201 (1), 92–100. doi: 10.1016/j.toxlet.2010.12.010
- Piersanti, A., Juganson, K., Mozzicafreddo, M., Wei, W., Zhang, J., Zhao, K., et al. (2021). Transcriptomic Responses to Silver Nanoparticles in the Freshwater Unicellular Eukaryote *Tetrahymena Thermophila*. *Environ. pollut.* 269, 115965. doi: 10.1016/j.envpol.2020.115965
- Quik, J. T., Vonk, J. A., Hansen, S. F., Baun, A. and Van De Meent, D. (2011). How to Assess Exposure of Aquatic Organisms to Manufactured Nanoparticles? *Environ. Int.* 37 (6), 1068–1077. doi: 10.1016/j.envint.2011.01.015
- Repka, S., Walls, M. and Ketola, M. (1995). Neck Spine Protects *Daphnia Pulex* From Predation by *Chaoborus*, But Individuals With Longer Tail Spine are at a Greater Risk. *J. Plankton Res.* 17 (2), 393–403. doi: 10.1093/plankt/17.2.393
- Rotini, A., Tornambè, A., Cossi, R., Iamunno, F., Benvenuto, G., Berducci, M. T., et al. (2017). Salinity-Based Toxicity of CuO Nanoparticles, CuO-Bulk and Cu Ion to *Vibrio Anguillarum*. *Front. Microbiol.* 8. doi: 10.3389/fmicb.2017.02076
- Scanlan, L. D., Reed, R. B., Loguinov, A. V., Antczak, P., Tagmount, A., Aloni, S., et al. (2013). Silver Nanowire Exposure Results in Internalization and Toxicity to *Daphnia Magna*. *ACS Nano* 7 (12), 10681–10694. doi: 10.1021/nn4034103
- Spicer, B. (2013). Assessing the Environmental Consequences of CO₂ Leakage From Geological CCS: Generating Evidence to Support Environmental Risk Assessment. *Mar. pollut. Bull.* doi: 10.1016/j.marpollbul.2013.05.044
- Trotter, B., Otte, K. A., Schoppmann, K., Hemmersbach, R., Fröhlich, T., Arnold, G. J., et al. (2015). The Influence of Simulated Microgravity on the Proteome of *Daphnia Magna*. *NPJ Microgravity* 1 (1), 15016. doi: 10.1038/npjmgrav.2015.16
- Volker, C., Boedicker, C., Daubenthaler, J., Oetken, M. and Oehlmann, J. (2013). Comparative Toxicity Assessment of Nanosilver on Three *Daphnia* Species in Acute, Chronic and Multi-Generation Experiments. *PLoS One* 8 (10). doi: 10.1371/journal.pone.0075026

- Wang, Z., Wang, Y. and Yan, C. (2016). Simulating Ocean Acidification and CO₂ Leakages From Carbon Capture and Storage to Assess the Effects of pH Reduction on Cladoceran *Moina Mongolica* Daday and its Progeny. *Chemosphere* 155, 621–629. doi: 10.1016/j.chemosphere.2016.04.086
- Wiesenthal, A., Hunter, L., Wang, S., Wickliffe, J. K. and Wilkerson, M. (2011). Nanoparticles: Small and Mighty. *Int. J. Dermatol.* 50 (3), 247–254. doi: 10.1111/j.1365-4632.2010.04815.x
- Yung, M. M. N., Kwok, K. W. H., Djurišić, A. B., Giesy, J. P. and Leung, K. M. Y. (2017). Influences of Temperature and Salinity on Physicochemical Properties and Toxicity of Zinc Oxide Nanoparticles to the Marine Diatom *Thalassiosira Pseudonana*. *Sci. Rep.* 7 (1), 3662. doi: 10.1038/s41598-017-03889-1
- Yung, M. M. N., Wong, S. W. Y., Kwok, K. W. H., Liu, F. Z., Leung, Y. H., Chan, W. T., et al. (2015). Salinity-Dependent Toxicities of Zinc Oxide Nanoparticles to the Marine Diatom *Thalassiosira Pseudonana*. *Aquat. Toxicol.* 165, 31–40. doi: 10.1016/j.aquatox.2015.05.015
- Zhu, X., Zhou, J. and Cai, Z. (2011). TiO₂ Nanoparticles in the Marine Environment: Impact on the Toxicity of Tributyltin to Abalone (*Haliotis Diversicolor Supertexta*) Embryos. *Environ. Sci. Technol.* 45 (8), 3753–3758. doi: 10.1021/es103779h
- Zuykov, M., Pelletier, E. and Demers, S. (2011). Colloidal Complexed Silver and Silver Nanoparticles in Extrapallial Fluid of *Mytilus Edulis*. *Mar. Environ. Res.* 71 (1), 17–21. doi: 10.1016/j.marenvres.2010.09.004

Conflict of Interest: The authors declare that the research was conducted in the absence of any commercial or financial relationships that could be construed as a potential conflict of interest.

Publisher's Note: All claims expressed in this article are solely those of the authors and do not necessarily represent those of their affiliated organizations, or those of the publisher, the editors and the reviewers. Any product that may be evaluated in this article, or claim that may be made by its manufacturer, is not guaranteed or endorsed by the publisher.

Copyright © 2022 Huang, Li and Lin. This is an open-access article distributed under the terms of the Creative Commons Attribution License (CC BY). The use, distribution or reproduction in other forums is permitted, provided the original author(s) and the copyright owner(s) are credited and that the original publication in this journal is cited, in accordance with accepted academic practice. No use, distribution or reproduction is permitted which does not comply with these terms.